J Artif Organs (2008) 11:123–129
DOI 10.1007/s10047-008-0416-5

ORIGINAL ARTICLE

Christoph L. Bara, MD · Janko F. Verhey, PhD

Simulation of the fluid dynamics in artificial aortic roots: comparison of two different types of prostheses

Abstract As a consequence of the growing number of elderly people, the incidence of degenerative aortic diseases continues to increase. Often, artificial aortic roots are needed to replace the native tissue. Some physical characteristics of the artificial aortic root, however, are quite different from native aorta and need to be optimized. The supposed benefit of a prosthesis with artificial sinuses of Valsalva could first be checked by numerical calculations. Two simplified base geometries were used for simulating the flow and pressure distributions, especially in the coronary arteries. One model approximates the ascending aorta as a tube, and the other uses a design with toroidal dilation of the aortic root to approximate the native geometry of the sinuses of Valsalva. The flow and pressure distributions in both models were compared in the ascending aorta as well as in the right and the left coronary arteries. Both the pressure and the velocity distribution in the coronary artery region were not significantly higher in the model with the sinus design compared to the tube model. The sinus design only slightly increased the mean pressures and the velocities in both the ascending aorta and in the coronary arteries. Higher pressure in the coronary arteries should improve the blood circulation and decrease the risk of a surgery-related coronary incident. The sinus design did not show the hoped-for benefits, and therefore it is only a minor factor in optimizing future aortic root prostheses.

Received: January 20, 2008 / Accepted: June 5, 2008

C.L. Bara (✉)
Department of Cardiac, Thoracic, Transplantation and Vascular Surgery, Hannover Medical School (OE6210), Carl-Neuberg-Str. 1, D-30625 Hannover, Germany
Tel. +49-511-532-6310; Fax +49-511-532-6309
e-mail: bara.christoph@mh-hannover.de

J.F. Verhey
MVIP Imaging Products GmbH, Nörten-Hardenberg, Germany

J.F. Verhey
Department of Medical Informatics, University Hospital Göttingen, Göttingen, Germany

Key words Hemodynamics · Coronary circulation · Computer modeling · Aortic surgery · Aortal prosthesis

Introduction

Aortic surgery has rapidly developed in recent years.[1–3] The growing number of elderly patients and the increasing incidence of degenerative aortic disease has stimulated the search for a gold standard treatment. New techniques for root replacement, e.g., the valve-sparing option described by David and Feindel[4] and the remodeling technique first described by Yacoub et al.,[5] are gaining wide attention and increasing acceptance. Both of these techniques require, however, a structurally intact aortic valve that must be suitable for reconstruction. Therefore, beside valve reconstruction, the standard composite root replacement using a Dacron tube with a mechanical valve still has a place in treatment of patients with aortic aneurysm.[6,7] In this type of surgery, the aortic root is replaced and the coronary arteries are reimplanted into the artificial tube. Some physical characteristics of the tube, however, are quite different to that of the native aorta. One of the most important differences is the lack of elasticity of the wall and, most obviously, the replacement aorta has a constant diameter over its whole length. In contrast, native aorta is normally bulbous at its root, i.e., until 4–5 cm above the valve it is pear-shaped and thus wider than the rest of the aorta. In addition, the wall is characterized by its great flexibility and distensibility, and these are crucial to its normal function.[8,9] The functional consequence of this structure, the so called Windkessel (compression chamber) mechanism, optimizes the blood flow and causes a continuous aortic flow despite the pulsatile nature of cardiac output.[10] Therefore, one of the main objectives in improving the characteristics of aortic prostheses is the development of a tube with some kind of a buffer similar to the human aortic root. Since there is little data regarding the recommended form and dimensions of the prosthesis, it would be of great interest to examine the influence of different lengths and widths and of the degree of

curvature of the artificial aortic root on the quality of blood flow. On the other hand, the benefit of a prosthesis with some kind of artificial sinuses of Valsalva is still not clearly documented, especially for the coronary arteries.[11] The aim of this study was to compare the flow characteristics of two aortic root models in an experimental computer simulation and to discover if the sinus design might be superior in terms of coronary flow.

Computational fluid dynamics (CFD) as a computational technology provides detailed performance assessment for a design and helps to reduce the need for costly experimentation. CFD enables sophisticated analysis to predict fluid flow behavior as well as heat transfer, mass transfer (e.g., perspiration, dissolution), phase change (e.g., freezing, boiling), chemical reaction (e.g., combustion), mechanical movement (e.g., impeller turning), and stress or deformation of a related structure. CFD allows the user to build a computational model that represents a system or device (e.g., the aortic root); then fluid flow physics[12] is applied to the device, and the software outputs a prediction of the fluid dynamics.

The use of CFD analysis even streamlines attempts to design and manufacture total artificial hearts (TAHs).[13,14] In this undertaking, the cardiovascular simulation is a coupled problem.[15] Not only is blood an inhomogeneous, anisotropic, non-Newtonian fluid, but also the boundaries of the flow, (the arteries, veins, and heart) are not rigid, and in many instances, these factors can have a pronounced effect on the flow. As a consequence, CFD analysis is basically used to provide an efficient method of carrying out sensitivity studies on key design parameters for selected parts of the heart. In the past, native as well as artificial geometries of ventricles,[16–18] valves and leaflets,[19–23] and vessels[24] were investigated and modeled. A good recent overview is given by Yoganathan et al.[25]

Such analyses can identify which parameters are the most significant for device design. Flow modeling provides engineers with the ability to accurately determine the performance of design concepts, reducing the need for physical testing and the building of prototypes. In this article we focus on the design of an aortic root prosthesis. To the knowledge of the authors, very few studies mention the aortic root and ascending aorta region or include them in their models.[26–33] Yet in 1997, Makhijani et al.[29] emphasized that the computer model has potential for being a powerful design tool for bioprosthetic aortic valves. This is an open challenge. None of the above-mentioned reports deals with the development of new and optimized designs of aortic root prostheses.

Methods

The simplified base geometry of the two prostheses described in this article was generated from real anatomical geometries similar to the models used in clinical practice. The parameters of the two base models are described in Fig. 1. One of the base models was created without a sinus design (model M1) and the other model has a sinus design (model M2). All the values were set according to average anatomical findings and could be modified in the model. On the assumption that the influence of a given aortic valve is essentially the same in both types of prostheses, i.e., with or

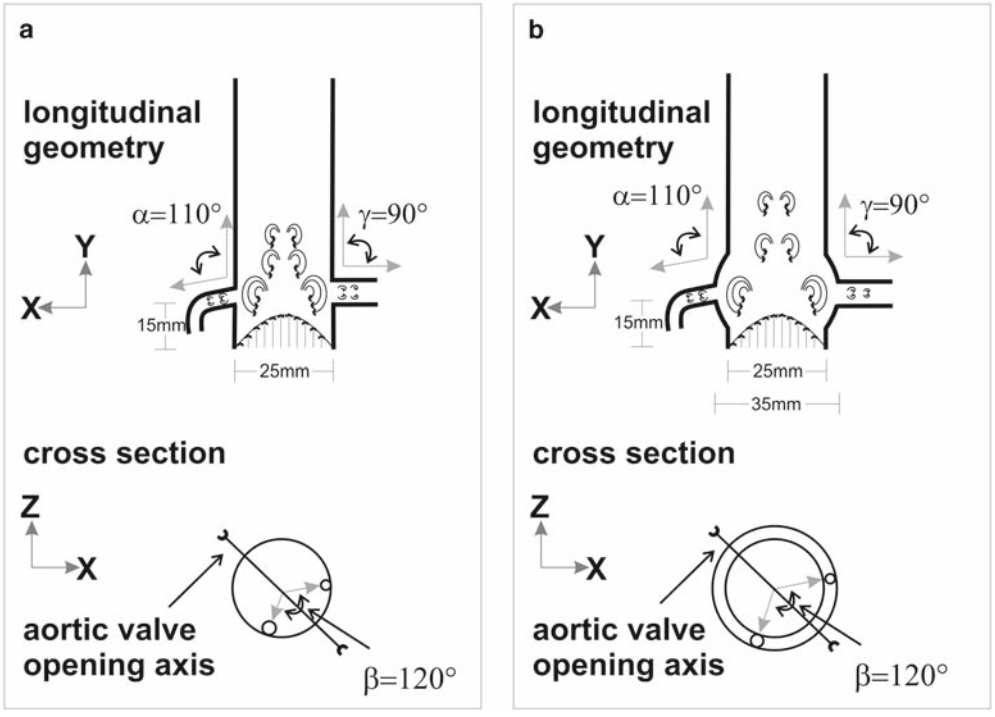

Fig. 1. Prosthesis model geometries showing the straight tube model M1 (**a**) and model M2 with a sinus design (**b**)

without the sinus design, we did not additionally calculate the flow across the valve.

Both models have in common the diameters of the inlet (the aortic valve) and the outlets (the ascending aorta and the left and the right coronary arteries). A diameter of 25 mm was set at the base of the aortic valve. The diameter of the left main coronary artery was set at 4 mm and that of the right coronary artery at 3 mm. The ascending part of the aorta had a diameter of 25 mm. The coronary arteries were placed at a distance of 15 mm above the aortic valve. In the model, the left main coronary artery is straight, has a length of 10 mm, and a coronary angle γ of 90°. The right coronary artery has a curvature of 90°, and at a length of 3 mm, the coronary angle α was set at 110°. The angle between the two coronary arteries was set at 120° (Fig. 1, lower part).

For model M2, the sinus design was approximated by a toroidal shape with an outer diameter of 35 mm and a height in the longitudinal *y*-axis of 10 mm (Fig. 1 and Fig. 2). In order to have comparable models, the overall lengths of the two models were the same. No geometrical parameter was modified in this study.

The model idealizes the fluid dynamics by assuming a laminar flow for the velocity profile. The parameters, especially the volume flow l_V, follow the law of Hagen–Poiseuille:

$$l_V = \frac{\pi \cdot r^4_{AorticValve}}{8 \cdot \eta \cdot l} \Delta p \qquad (1)$$

The blood viscosity η used in the modeling was $\eta = 3.5 \cdot 10^{-3}$ Pa·s, 1 and r are the length and radius of the duct, Δp is the pressure drop, π is the mathematical constant (approximately 3.1416). The parameter sets for both geometry and fluid dynamics idealize the real anatomy and physiology. In particular, this means:

- The walls of the models are rigid.
- Blood is treated as a noncompressible fluid. As a result the continuous mass flow equation can be applied.
- Capillarity is neglected.
- Blood pressure is assumed to be homogeneous, as it would occur in a person lying down at normal atmospheric pressure.
- The density of blood is assumed to be constant at 1060 kg/m^3.
- In reality, the viscosity of blood depends on many factors such as temperature, velocity, and hemocomposition. In this model, blood was assumed to be an ideal Newtonian fluid so the viscosity does not depend on temperature and volume flow. The radial component of the law of Hagen–Poiseuille was therefore neglected.
- The flow distribution at the inlet of the aortic valve region was idealized to a laminar flow. Turbulent components were calculated inside the model.
- Effects on the volume flow caused by the aortic valve (e.g., jet-type flow) were neglected.

The volume flow rates were set according to the values in Table 1. An average continuous value (83.33 ml/s) corresponding to physiological findings for a blood volume flow of 5 l/min was assumed for the inlet at the aortic valve. During the heart cycle, the pressure in the ascending aorta physiologically varies in the range from around 75 mmHg (99.99 hPa) to around 130 mmHg (173.32 hPa). For our calculations, we assumed an average pressure of 100 mmHg (133.32 hPa).

The base geometries for both models were generated with the standard finite element program ABAQUS 6.5.1 (SIMULIA previously ABAQUS Inc., Providence, USA) running on a Sun-Server Sun E10000. They are shown in Fig. 2. The fluid dynamic calculations were carried out with Fluent Flow Wizard 1.0.8 (ANSYS Inc., Lebanon, USA) running on a Windows XP Professional-based standard workstation (CPU 1.4 MHz, 500 MB RAM).

Results

The simulation results for pressure and velocity distribution are shown in Figs. 3 and 4. Longitudinal profiles are presented in Fig. 3 and cross-sectional profiles are shown in Fig. 4. Detailed quantified results for the pressure are given in the Table 2, and Table 3 gives the results for the velocities. All tables give results for the boundaries – the inlet and the outlets – for both models to allow comparison.

In all images of Fig. 3, the assumed idealized laminar flow at the aortic valve region is visible as a homogeneous

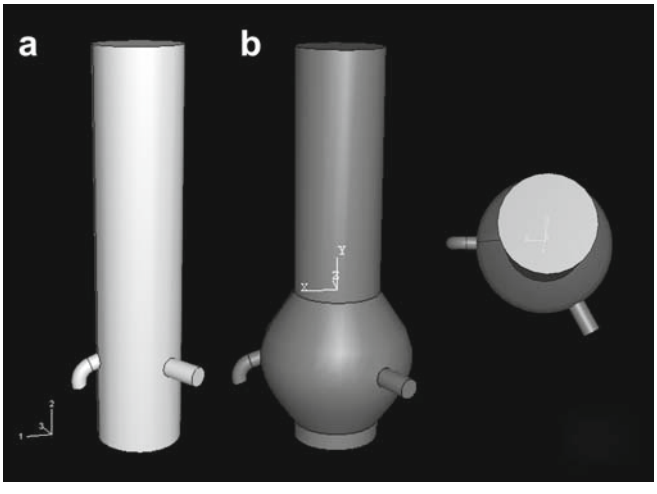

Fig. 2. Modeled aortic ducts show the geometry of the straight tube (**a**) and the geometry with a sinus design (**b**) from two different points of view

Table 1. Boundary conditions for the volume flow rate

Boundary	Type	Volume flow rate (ml/s)
Aortic valve (inlet)	Inlet	83.33
Right coronary artery	Outlet	1.61
Left coronary artery	Outlet	2.55
Ascending aorta (outlet)	Outlet	79.17

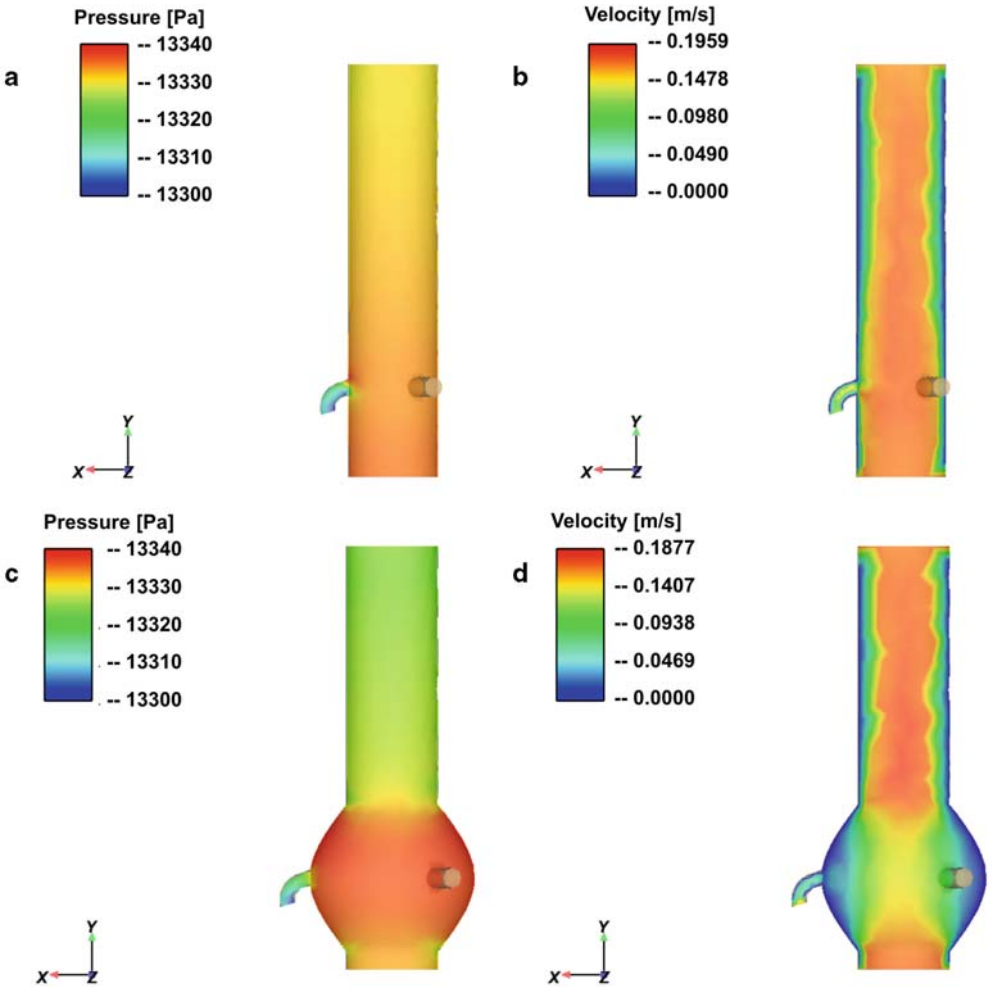

Fig. 3. Longitudinal profiles of pressure (**a,c**) and velocity (**b,d**). The *upper* parts illustrate the flow for model M1 and the *lower* parts show the corresponding profiles for model M2. Turbulent components are observed, especially regarding the color code transition from green to orange (**b,d**)

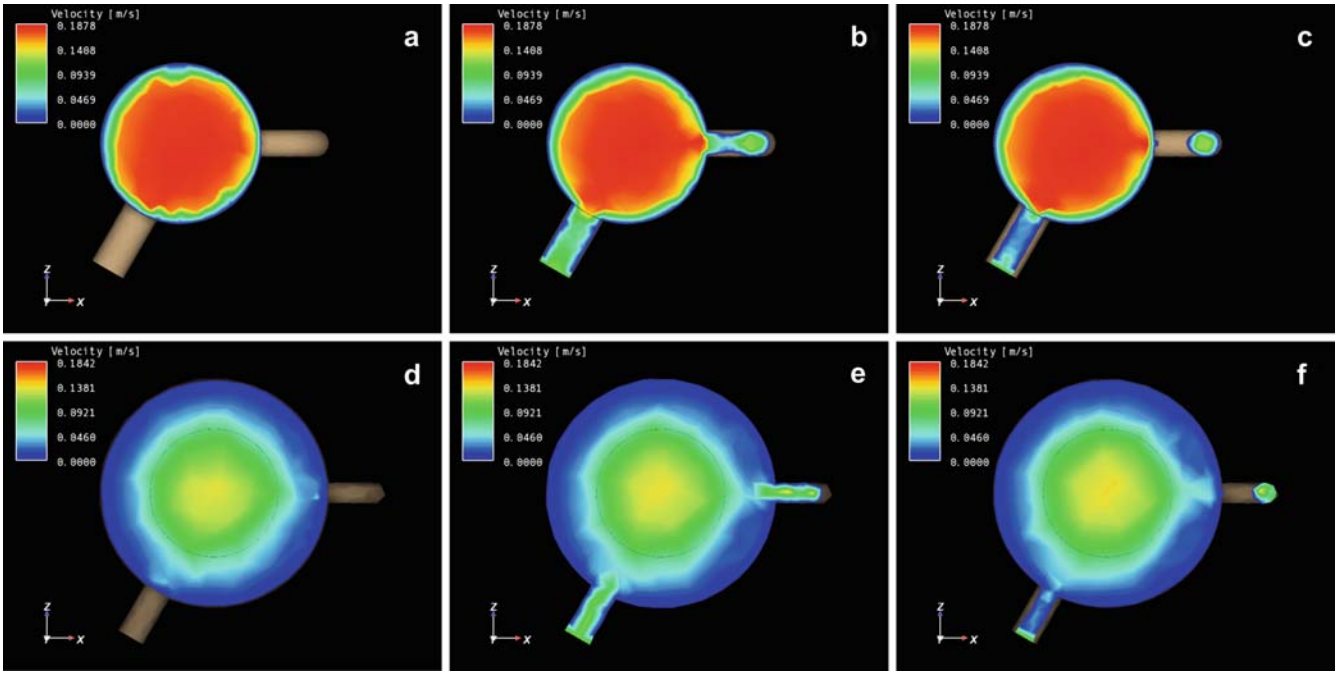

Fig. 4. Cross-sectional velocity distributions for model M1 (**a**–**c**) and model M2 (**d**–**f**). **b** and **e** show the pressure distribution in the coronary arteries. Cross sections **a** and **d** are located above the coronary arteries and **c** and **f** are located below the coronary arteries

Table 2. Detailed pressures for both models

Location	M1 pressure (hPa)			M2 pressure (hPa)		
	Min	Max	Average	Min	Max	Average
Aortic valve (inlet)	100.02	173.36	133.36	99.99	173.35	133.34
Right coronary artery	99.59	173.02	132.98	99.69	173.10	133.06
Left coronary artery	99.77	173.14	133.12	99.90	173.23	133.23
Ascending aorta (outlet)	99.93	173.28	133.27	99.90	173.24	133.24

Table 3. Flow velocities

Location	Mean velocity (m/s)		
	M1	M2	Δ (M1–M2)
Aortic valve (inlet)	0.174	0.171	0.003
Right coronary artery	0.121	0.142	–0.021
Left coronary artery	0.108	0.113	–0.005
Ascending aorta (outlet)	0.167	0.167	0.000

color distribution. Turbulent components are observed above the coronary artery region for both models (Figs. 3b,d). At the center of the aortic duct the velocity is significantly higher than at the borders of the tube. The region surrounding the coronary arteries is of special interest. In this region, the pressure and velocity distributions differ between model M1 and M2. The decrease in pressure in model M1 is continuous and depends on the length of the tube. The distortion of the pressure distribution caused by the coronary arteries seems to be negligible (Fig. 3a). A similar effect is noted in the velocity distribution of model M1; generally, the turbulence increases in the flow direction but the overall velocity distribution profile does not change very much (Fig. 3b). The absolute values of pressure and velocity in the coronary artery region do not differ significantly between model M1 and M2. (Fig. 4, Tables 2 and 3).

In the region above the coronary arteries, the relative pressure distribution is different in the two models. Whereas the pressure in model M1 continuously decreases along the length of the tube (Fig. 3a), Fig. 3c (model M2) clearly shows a discontinuous change at the end of the pseudo-sinus region. The pressure above the pseudo-sinus region is generally lower in model M2 than in model M1. The average pressure at the outlet of the ascending aorta in model M1 is 4.7 Pa (Table 2) lower than the assumed overall average blood pressure of 133.32 hPa (= 100 mmHg). This difference is smaller than in model M2, where the pressure difference is 8.5 Pa (Table 2).

The velocity distributions (Figs. 3b,d) show that in the coronary artery region the velocity is lower in model M2 than in model M1. Figure 4 shows the cross-sectional velocity distribution at three different levels: above, at, and below the level of the coronary arteries. In model M1 the velocity at the center of the model in the coronary artery cross section (Fig. 4b) is about 0.19 m/s. The velocity at the same region in Fig. 4e for model M2 is unexpectedly lower at about 0.14 m/s.

Discussion

The physiologic function of the aorta is influenced by its pear-shaped root (due to the presence of the sinuses of Valsalva) as well as by the distensibility and elasticity of the wall. All of these factors contribute to the so-called Windkessel effect, which results in nearly continuous blood flow despite the pulsatile nature of the cardiac output. The contribution to this effect made by the sinuses of Valsalva is not known; their absence in aortic root prostheses makes the blood flow less favorable. The aim of this study was to evaluate the possible improvement in the flow resulting from a new aortic root prosthesis with a pseudo-sinus feature.

In order to minimize the risk of coronary incidents, any surgical intervention should lead to an optimized pressure and velocity distribution in the coronary arteries. The higher the pressure and the velocity in the critical coronary artery regions, the lower would be the risk of significant coronary insufficiency. The results of the simulations show only a slightly increased pressure and no increase in velocity for the sinus design of model M2 compared to the standard duct. Our calculations show that the supposed benefit is marginally observed, but it is not as large an effect as was anticipated. To the authors' knowledge, there is only a single previous investigation of the coronary flow after aortic root replacement, that performed by De Paulis et al.[11] They examined patients with both a standard cylindrical Dacron conduit and with the sinus conduit 1 year after surgery. No influence of the pseudo-sinuses of Valsalva was found on the coronary flow. This corresponds to our findings. They did, however, find a greater diastolic component of the flow in the group of patients with the sinus-design conduit and suggested that the coronary flow pattern may be affected by the presence of the sinuses. Our simulations, inspired among others by these findings, could not corroborate these suggestions and thus provide a theoretical confirmation. The results, however, must be examined in light of further clinical investigations considering different prosthesis designs.

The model geometries we used for the fluid dynamics simulations idealize and simplify radically the real anatomy and physiology. In real geometries, the walls of the models are not rigid, the blood pressure is not homogeneous, and the flow is turbulent. For this study, simplifying assumptions were made because the effect should be similar on both models and should thus allow valid results to be obtained. Therefore, we neglected these effects in this first simulation

and made the assumptions described in detail in the Methods section.

Future studies could build more complicated computational fluid dynamics models: additional geometric boundary conditions could be added, physiological blood parameters could be adopted, and the flow characteristic could be enhanced by moving from the steady assumption to a pulsatile flow characteristic. This should lead to even more realistic values and allow optimization of the size of the artificial sinuses of Valsalva.

One of these effects might consist of considering pulsatile pressure distributions as well as the pressure losses throughout the tube length. Such a pressure loss is a logical consequence of the law of Hagen–Poiseuille, but it differs for turbulent flows as well as for modifications of the pipe friction values due to uneven inner diameters of the vessel.

The influence of the aortic valve on coronary flow is probably similar in both types of root prostheses, although it might differ depending on the type of the valve. Further examination of this effect according to the configuration of the aortic valve may provide additional information. In general, however, the results should not be significantly influenced by the above-mentioned factors. Our study provides initial experimental proof suggesting that model prostheses with the sinus design are comparable to models without the sinus design.

It is of great importance to optimize the blood flow for all vascular prostheses, but it is especially important in prostheses of the aortic root because of the crucial role played in the cardiovascular system. Computational methods are nowadays accepted as powerful tools for quantifying blood flow in arteries as well as for disease research, medical device design, and treatment planning. Nevertheless, some further clinical studies are required to confirm these results in vivo. It would be particularly helpful because the standard Dacron straight duct so far mainly used in interventions where artificial aortic root prosthesis are implanted seems to produce similar results to the model with the sinus design. On the other hand, although prostheses with pseudosinuses of Valsalva are already available, there is no evidence concerning the best size and form of the prosthesis, nor is there evidence about any benefits compared to the straight duct prosthesis. Perhaps some other optimizable factors might be found in the future. Furthermore, since it is reasonable to assume that the Windkessel effect influences the function of many organs through the resulting sustained perfusion pressure, it would be interesting to investigate this feature as well. We intend to at least study its affect on the cerebral circulation. It seems to be especially important because of the increasing implantation rate of nonpulsatile assist devices.

Conclusion

The simulation of the fluid dynamics in model aortic prostheses shows that the sinus design for the artificial aortic root does not significantly increase the pressures and the velocities in the coronary arteries.

References

1. Kallenbach K, Karck M, Pak D, Salcher R, Khaladj N, Leyh R, Hagl C, Haverich A. Decade of aortic valve-sparing reimplantation: are we pushing the limits too far? Circulation 2005;112(suppl 9):I253–259
2. Kallenbach K, Karck M, Leyh RG, Hagl C, Walles T, Harringer W, Haverich A. Valve-sparing aortic root reconstruction in patients with significant aortic insufficiency. Ann Thorac Surg 2002;74:1765–1768; discussion S92–99
3. Karck M, Kallenbach K, Hagl C, Rhein C, Leyh R, Haverich A. Aortic root surgery in Marfan syndrome: comparison of aortic valve-sparing reimplantation versus composite grafting. J Thorac Cardiovasc Surg 2004;127:391–398
4. David TE, Feindel CM. An aortic valve-sparing operation for patients with aortic incompetence and aneurysm of the ascending aorta. J Thorac Cardiovasc Surg 1992;103:617–622
5. Yacoub M, Fagan A, Tassano P, Radley-Smith R. Result of valve-conserving operations for aortic regurgitation. Circulation 1983; 68(suppl 3):321
6. Mingke D, Dresler C, Stone CD, Borst H. Composite graft replacement of the aortic root in 335 patients with aneurysm or dissection. Thorac Cardiovasc Surg 1998;46:12–19
7. Gott VL, Gillinov AM, Pyeritz RE, Cameron DE, Reitz BA, Greene PS, Stone CD, Ferris RL, Alejo DE, McKusick VA. Aortic root replacement. Risk factor analysis of a seventeen-year experience with 270 patients. J Thorac Cardiovasc Surg 1995;109: 536–545
8. Isselbacher EM. Diseases of the aorta. In: Braunwald E, Zipes DP, Libby P (eds) Heart disease: a textbook of cardiovascular medicine, vol 2. 6th edn. Philadelphia: W.B. Saunders, 2001; 1422
9. Lindsay J, DeBakey ME, Beal AC. Diagnosis and treatment of diseases of the aorta. In: Schlant RC, Alexander RW (eds) Hurst's the heart: arteries and veins. 8th edn. New York: McGraw-Hill, 1994;2163
10. Schlant RC, Sonnenblick EH. Normal physiology of the cardiovascular system. In: Schlant RC, Alexander RW (eds) Hurst's the heart: arteries and veins. 8th edn. New York: McGraw-Hill, 1994; 139
11. De Paulis R, Tomai F, Bertoldo F, Ghini AS, Scaffa R, Nardi P, Chiariello L. Coronary flow characteristics after a Bentall procedure with or without sinuses of Valsalva. Eur J Cardiothorac Surg 2004;26:66–72
12. Granger RA. Fluid mechanics. New York: Dover Publications, 1995
13. Gursahani S, Ponce E, Nagaraju M, Tatke S. Biofluid dynamics of the artificial heart. In: Goyal MR (ed) Congress on Biofluid Dynamics of Human Body Systems at Biomedical Engineering. Miami: 2003;B1–25
14. Shim EB, Yeo JY, Ko HJ, Youn CH, Lee YR, Park CY, Min BG, Sun K. Numerical analysis of the three-dimensional blood flow in the Korean artificial heart. Artif Organs 2003;27:49–60
15. Pekkan K, de Zelicourt D, Ge L, Sotiropoulos F, Frakes D, Fogel MA, Yoganathan AP. Physics-driven CFD modeling of complex anatomical cardiovascular flows – a TCPC case study. Ann Biomed Eng 2005;33:284–300
16. Song X, Wood HG, Olsen D. Computational fluid dynamics (CFD) study of the 4th-generation prototype of a continuous flow ventricular assist device (VAD). J Biomech Eng 2004;126:180–187
17. Watanabe H, Hisada T, Sugiura S, Okada J, Fukunari H. Computer simulation of blood flow, left ventricular wall motion and their interrelationship by fluid–structure interaction finite element method. JSME Int J Series C 2002;45:1003–1012
18. Throckmorton AL, Lim DS, McCulloch MA, Jiang W, Song X, Allaire PE, Wood HG, Olsen DB. Computational design and experimental performance testing of an axial-flow pediatric ventricular assist device. ASAIO J 2005;51:629–635

19. Yin W, Alemu Y, Affeld K, Jesty J, Bluestein D. Flow-induced platelet activation in bileaflet and monoleaflet mechanical heart valves. Ann Biomed Eng 2004;32:1058–1066
20. Ge L, Leo HL, Sotiropoulos F, Yoganathan AP. Flow in a mechanical bileaflet heart valve at laminar and near-peak systole flow rates: CFD simulations and experiments. J Biomech Eng 2005; 127:782–797
21. Black MM, Drury PJ. Mechanical and other problems of artificial valves. Curr Top Pathol 1994;86:127–159
22. Choi CR, Kim CN. Analysis of blood flow interacted with leaflets in MHV in view of fluid–structure interaction. KSME J 2001;15: 613–622
23. De Hart J, Peters GWM, Schreurs PJG, Baaijens FPT. A three-dimensional computational analysis of fluid–structure interaction in the aortic valve. J Biomech 2003;36:103–112
24. Grigioni M, Daniele C, Morbiducci U, D'Avenio G, Di Benedetto G, Del Gaudio C, Barbaro V. Computational model of the fluid dynamics of a cannula inserted in a vessel: incidence of the presence of side holes in blood flow. J Biomech 2002;35:1599–1612
25. Yoganathan AP, Chandran KB, Sotiropoulos F. Flow in prosthetic heart valves: state-of-the-art and future directions. Ann Biomed Eng 2005;33:1689–1694
26. Leuprecht A, Perktold K, Kozerke S, Boesiger P. Combined CFD and MRI study of blood flow in a human ascending aorta model. Biorheology 2002;39:425–429
27. Saber NR, Wood NB, Gosman AD, Merrifield RD, Yang G-Z, Charrier CL, Gatehouse PD, Firmin DN. Progress towards patient-specific computational flow modeling of the left heart via combination of magnetic resonance imaging with computational fluid dynamics. Ann Biomed Eng 2003;31:42–52
28. Sankaranarayanan M, Chua LP, Ghista DN, Tan YS. Computational model of blood flow in the aorto-coronary bypass graft. Biomed Eng Online 2005;4:14
29. Makhijani VB, Yang HQ, Dionne PJ, Thubrikar MJ. Three-dimensional coupled fluid–structure simulation of pericardial bioprosthetic aortic valve function. ASAIO J 1997;43:M387–392
30. May-Newman K, Hillen B, Dembitsky W. Effect of left ventricular assist device outflow conduit anastomosis location on flow patterns in the native aorta. ASAIO J 2006;52:132–139
31. May-Newman KD, Hillen BK, Sironda CS, Dembitsky W. Effect of LVAD outflow conduit insertion angle on flow through the native aorta. J Med Eng Technol 2004;28:105–109
32. Kiris C, Kwak D, Rogers S, Chang ID. Computational approach for probing the flow through artificial heart devices. J Biomech Eng 1997;119:452–460
33. King MJ, Corden J, David T, Fisher J. A three-dimensional, time-dependent analysis of flow through a bileaflet mechanical heart valve: comparison of experimental and numerical results. J Biomech 1996;29:609–618